Geochemistry Geophysics Geosystems G3

Article
Volume 14, Number 10
2 October 2013
doi: 10.1002/ggge.20257
ISSN: 1525-2027

Published by AGU and the Geochemical Society

The Giant Pacific Oyster (*Crassostrea gigas*) as a modern analog for fossil ostreoids: Isotopic (Ca, O, C) and elemental (Mg/Ca, Sr/Ca, Mn/Ca) proxies

Clemens V. Ullmann
Institut für Geologische Wissenschaften, Freie Universität Berlin, Berlin, Germany

Department of Geosciences and Natural Resource Management and Nordic Center for Earth Evolution (NordCEE), University of Copenhagen, Øster Voldgade 10, 1350 Copenhagen, Denmark (c.v.ullmann@gmx.net)

Florian Böhm
Geomar Helmholtz-Zentrum für Ozeanforschung Kiel, Kiel, Germany

Rosalind E.M. Rickaby
Department of Earth Sciences, University of Oxford, Oxford, UK

Uwe Wiechert
Freie Universität Berlin, Institut für Geologische Wissenschaften, Berlin, Germany

Christoph Korte
Freie Universität Berlin, Institut für Geologische Wissenschaften, Berlin, Germany

Department of Geosciences and Natural Resource Management and Nordic Center for Earth Evolution (NordCEE), University of Copenhagen, Copenhagen, Denmark

[1] Modern analogs are an essential part of palaeoclimate studies, because they provide the basis for the understanding of geochemical signatures of fossils. Ostreoids are common in many sedimentary sequences and because of their fast growth, high temporal resolution sampling of past seasonal variability is possible. Here, two shell structures of modern Giant Pacific Oysters (*Crassostrea gigas*), the chalky substance and foliate layers, have been sampled for trace element distributions (Mg, Sr, Mn) and stable isotope variability (C, O, Ca). Oxygen isotopes exhibit a clear seasonal signature. Mean carbon isotope values of different oysters agree within 0.1‰, but ontogenic variability is complicated by shell growth patterns and potential small vital effects. The calcium isotope ratios are found to be constant throughout ontogeny within analytical precision at a value of $\delta^{44/40}Ca = 0.68 \pm 0.16$‰ (2 sd) SRM–915a which is consistent with other bivalve species. Calcium isotope ratios in oyster shell material might thus be a possible proxy for palaeo seawater calcium isotope ratios. Element/Ca ratios are significantly higher in the chalky substance than in the foliate layers and especially high Sr/Ca and Mn/Ca ratios are observed for the first growth season of the oysters. Mg/Ca ratios in the chalky substance show a negative correlation with $\delta^{18}O$ values, compatible with a temperature dependence, whereas this correlation is absent in the foliate layers. Seasonal changes of Sr/Ca are controlled by metabolic processes, whereas for Mn/Ca an additional environmental control is evident.

Components: 7,701 words, 7 figures.

Keywords: *Crassostrea gigas*; shell chemistry; modern analog.

Index Terms: 0419 Biomineralization: Biogeosciences; 0454 Isotopic composition and chemistry: Biogeosciences; 0424 Biosignatures and proxies: Biogeosciences; 1041 Stable isotope geochemistry: Geochemistry; 1050 Marine geochemistry: Geochemistry; 1065 Major and trace element geochemistry: Geochemistry; 4835 Marine inorganic chemistry: Oceanography: Biological and Chemical; 4845 Nutrients and nutrient cycling: Oceanography: Biological and Chemical; 4850 Marine organic chemistry: Oceanography: Biological and Chemical; 4870 Stable isotopes: Oceanography: Biological and Chemical.

Received 28 February 2013; **Revised** 25 July 2013; **Accepted** 16 August 2013; **Published** 2 October 2013.

Ullmann, C. V., F. Böhm, R. E. M. Rickaby, U. Wiechert, and C. Korte (2013), The Giant Pacific Oyster (*Crassostrea gigas*) as a modern analog for fossil ostreoids: Isotopic (Ca, O, C) and elemental (Mg/Ca, Sr/Ca, Mn/Ca) proxies, *Geochem. Geophys. Geosyst.*, *14*, 4109–4120, doi:10.1002/ggge.20257.

1. Introduction

[2] Stable isotope (Ca, O, C) and elemental (Mg/Ca, Sr/Ca, Mn/Ca) distribution patterns in shell materials of calcifying organisms are controlled by seawater chemistry and environmental conditions. This fact enables the reconstruction of past seawater conditions and palaeoenvironments from carbonate fossils, such as brachiopods, bivalve mollusks, belemnites, and foraminifers [e.g., *Buchardt*, 1978; *Veizer et al*., 1999; *Zachos et al*., 2001; *Steuber and Veizer*, 2002; *Farkaš et al*., 2007; *Prokoph et al*., 2008; *Blättler et al*., 2012]. Some of these organisms, however, show species dependent fractionations of isotope and element ratios (vital effects) during the formation of their shells. The extent of vital effects in ancient specimens can be addressed by investigations of phylogenetically related modern species, in culture or from the field. Such calibrations are essential, because element concentrations and isotopic ratios may be proxies for different environmental parameters, depending on the studied species [e.g., *Klein et al*., 1996; *Vander Putten et al*., 2000; *Lorrain et al*., 2005; *Freitas et al*., 2006; *Ford et al*., 2010; *Heinemann et al*., 2011; *Schöne et al*., 2011; *Freitas et al*., 2012].

[3] The biomineralization of oysters is of particular interest because of their large economic value [e.g., *Pauley et al*., 1988] but also because of their common occurrence as fossils in the sedimentary record [e.g., *Korte and Hesselbo*, 2011]. Numerous studies investigated aspects of biomineralization of oysters, focusing on the role of organic molecules [e.g., *Lee and Choi*, 2007; *Lee et al*., 2011; *Marie et al*., 2011], bulk shell and amino acid composition [*Almeida et al*., 1998] and element concentrations in foliate and prismatic layers [*Dauphin et al*., 2013]. Studies reporting both, isotopic and elemental compositions of oyster shell material, especially of the chalky substance, however, are rare (but see *Goodwin et al*. [2013]).

[4] Here we focus on oyster shells from a well monitored area, where environmental factors have been studied continuously for more than 20 years, so that external influences on the organism can be approximated. We present high resolution data sets for Mg/Ca, Sr/Ca, and Mn/Ca ratios as well as isotope ratios of C, O, and Ca in two different shell structures, the chalky substance and foliate layers. We show the primary variability of the chemical and isotopic composition and investigate, which information about past environments can potentially be derived from the analysis of the respective tracers.

2. Materials and Methods

[5] Oysters of the species *C. gigas* were sampled by Karsten Reise (Alfred Wegener Institute, Sylt) in the fall of 2007 from the List Tidal Basin, Germany (Figure 1a). This semienclosed basin, covering an area of about 400 km^2, is located in the Northern Wadden Sea and connected to the North Sea by a tidal inlet between the islands of Sylt, Germany and Rømø, Denmark (Figures 1a and 1b) [*van Beusekom et al*., 2008]. The specimens were sampled from a shallow subtidal oyster bank close to the Island of Sylt. Monthly measurements of water temperatures and salinities in the relevant time interval from 2003 to 2007 showed variations between 0.2 to 20.3°C and 27.2 to 31.4 psu [*van Beusekom et al*., 2008] (Figure 1c). The salinity changes are mainly controlled by discharge variations of the rivers Elbe and Weser [*van Beusekom et al*., 2008].

2.1. Shell Material

[6] Oysters are macrobenthic, filtering, and opportunistic suspension feeders [*Leal et al*., 2008;

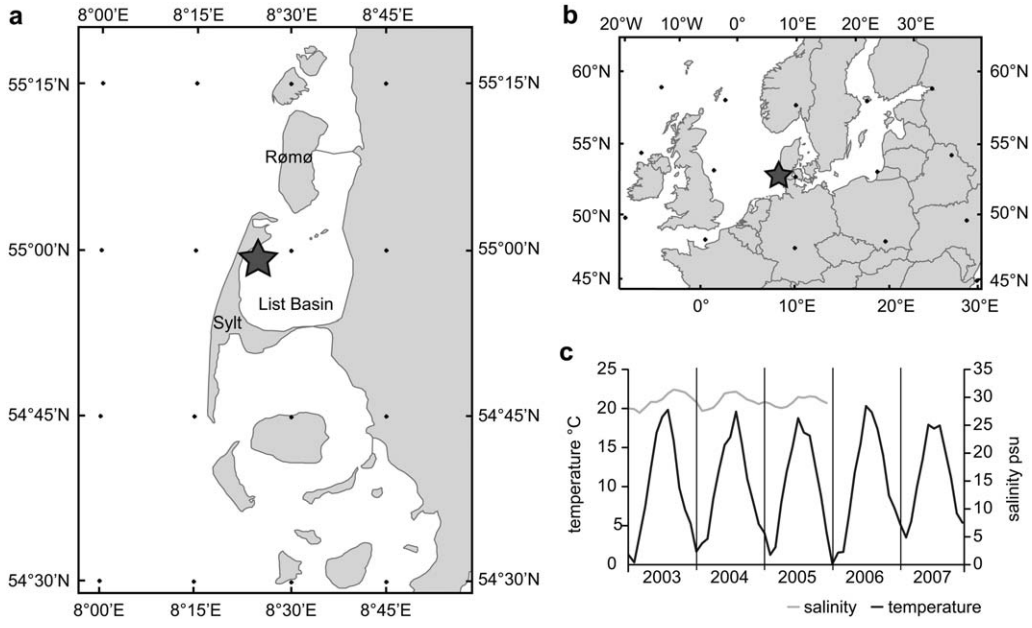

Figure 1. (a and b) Sample location in the List Basin. (c) Salinities and temperatures at the sample location with monthly resolution.

Dauphin et al., 2013]. They grow preferentially on hard substrates in estuaries in the intertidal and shallow subtidal zones [*Quayle*, 1969; *Pauley et al*., 1988] and prefer water temperatures of 4–24°C and salinities >20 psu [*Pauley et al*., 1988]. For a more comprehensive picture of oyster ecology, see *Quayle* [1969] and *Pauley et al*. [1988].

[7] Shells of juvenile and adult oysters consist mainly of calcite [*Lee et al*., 2006]. The calcitic part of the shell of *Crassostrea gigas* comprises the outermost prismatic layer, foliate layers, and chalky substance (Figure 2) [*Miyawaki*, 1954; *Carriker and Palmer*, 1979; *Carriker et al*., 1980; *MacDonald et al*., 2009; *Dauphin et al*., 2013]. The chalky substance (Figure 2a) is specific to oysters [*Dauphin et al*., 2013] and apparently an early feature of oyster evolution. Its presence has been inferred for Cretaceous [*Chinzei*, 1986; *Ayoub-Hannaa and Fürsich*, 2011] and even Jurassic oysters [*Komatsu et al*., 2002]. Contrasting to the network of microcrystalline calcite laths of the chalky substance, the foliate layers are composed of interfingering bladelike calcite crystals (Figures 2a and 2b; see also *Ullmann et al*. [2010]).

2.2. Sample Preparation

[8] The left valve of three shells was cut through the umbo and a ~2 mm thick section of the umbo was mounted on a glass slide with epoxy resin for further sampling (Figure 3). One of the investigated profiles stems from the same oyster that was

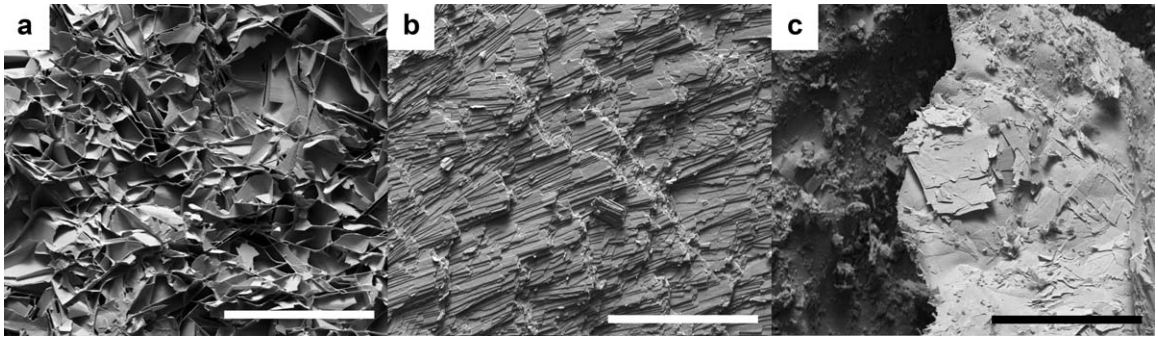

Figure 2. SEM images of shell structures of *C. gigas*: (a) chalky substance, (b) foliate layers, and (c) millimeter-sized sheet of organic material in contact with foliate layers. A thin package of foliate layers attached to the organic material is visible in the central part. Scale bars are 50 μm.

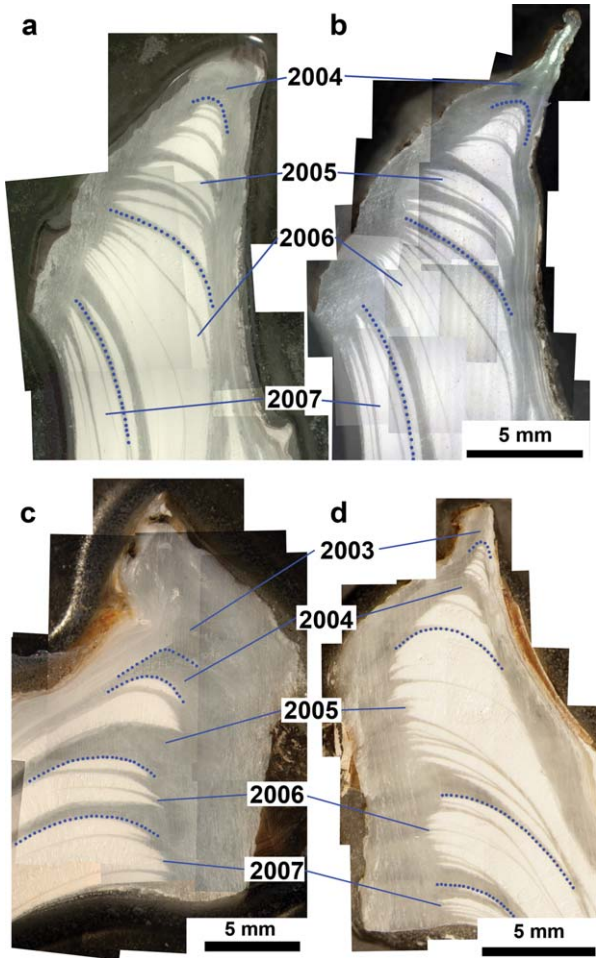

Figure 3. Sections through the umbo of the investigated specimens of *C. gigas*: (a) section of specimen vl used for this study, (b) parallel section of specimen vl studied by *Ullmann et al*. [2010], (c) section of specimen 8l, and (d) section of specimen 1l. Age estimates for the shell material are based on oxygen isotope results discussed in *Ullmann et al*. [2010] and in sections 3 and 4. Sample positions of the two profiles through specimen vl were correlated using growth bands. Dotted lines indicate approximate boundaries between growth bands attributed to different years.

analyzed by *Ullmann et al*. [2010] (Figures 3a and 3b). Foliate layers and chalky substance [*Carriker and Palmer*, 1979; *Carriker et al*., 1980] were sampled to assess the potential effects of the differing ultrastructure on the geochemical tracers. A total of 91, 110, and 70 samples, respectively, were taken along traces through the sections of specimens vl, 8l and 1l, with an average resolution of ~0.2 mm per sample. Aliquots were prepared by scratching shell calcite parallel to the growth bands using a stainless steel scalpel. Each sample was homogenized with a spatula and subdivided into subsamples for carbon and oxygen isotopic analyses and element ratio determinations. From 14 of the homogenized aliquots of specimen vl, calcium isotope ratios were analyzed.

2.3. Carbon and Oxygen Isotope Preparation

[9] The carbon and oxygen isotope measurements on specimen vl were carried out on ~100–500 µg sample powder using the MAT-253 THERMO^{TM} Finnigan Isotope Ratio Mass Spectrometer at the Freie Universität Berlin using the routines described in *Ullmann et al*. [2010]. The external reproducibility of the measurements was 0.07‰ (2 sd) for $\delta^{13}C$ and 0.12‰ (2 sd) for $\delta^{18}O$ as defined from the results for a laboratory reference material measured together with the samples ($n = 20$). The results were correlated with the higher resolution data set from *Ullmann et al*. [2010] by matching the growth bands of the investigated sections and assigning the new samples to the closest spaced sample from the higher resolution profile. No further adjustments in the spacing were applied. Carbon and oxygen isotope measurements of specimens 8l and 1l were conducted at the University of Copenhagen with a Micromass IsoPrime Isotope Ratio Mass Spectrometer, using the routines described in *Ullmann et al*. [2013]. Sample amounts were ~400–800 µg. The external reproducibility of the analyses is 0.08‰ (2 sd) for $\delta^{13}C$ and 0.16‰ (2 sd) for $\delta^{18}O$ as defined by multiple analyses of a laboratory reference material ($n = 56$).

2.4. Trace Element Preparation

[10] Splits for element ratio determinations of specimen vl were processed in the clean air laboratory of the Department of Earth Sciences, University of Oxford, UK. The carbonate powders were transferred to acid cleaned tubes and weighed. The material was reacted with 500 µL of 0.3 M HNO_3 and diluted with 0.3 M HNO_3 to a calculated concentration of 100 µg/g calcium. Aliquots were measured using a PESCIEX ELAN 6100 DRC Quadrupole ICP-MS at the University of Oxford analogous to the method described in *Ferguson et al*. [2008] using a standard sample bracketing protocol with a synthetic multielement solution as a reference material. The element concentrations of the calibration solution were measured against the Merck ICP multielement solution VI for accuracy control. Repeatability for the calibration solution is better than 4% for Mg/Ca and Sr/Ca ratios and better than 5% for Mn/Ca ratios (2 sd, $n = 113$).

[11] Element ratios of samples from specimens 8l and 1l were measured at the University of Copenhagen using an Optima 7000 DV ICP-OES. Sample powders were reacted with 0.2 M HNO_3 and Ca concentrations adjusted to a nominal concentration of 25 µg/g by dilution with 0.2 M HNO_3. Element concentrations were determined using a three-point calibration with two matrix matched synthetic calibration solutions and a blank solution. Spectral intensities of Ca (317.933 nm), Mg (280.271 nm), and Sr (407.771 nm) were analyzed in radial mode, while Mn (257.610 nm) was measured in axial mode for better sensitivity. Precision and accuracy of the analyses were determined by multiple measurements of JLs-1 (limestone). Repeatability was better than 2% for Mg/Ca and Sr/Ca ratios and better than 5% for Mn/Ca ratios (2 sd, $n = 24$). Average results of the element ratios of JLs-1 were 13.9 mmol/mol for Mg/Ca, 0.343 mmol/mol for Sr/Ca, and 29.8 µmol/mol for Mn/Ca, which compares to published values of 15.3 mmol/mol, 0.343 mmol/mol, and 30.0 µmol/mol, respectively [*Imai et al*., 1996].

2.5. Calcium Isotope Measurements

[12] Calcium isotope ratios were measured with a Finnigan Triton TI TIMS (Thermal Ionization Mass Spectrometer) at the Geomar Helmholtz-Zentrum für Ozeanforschung Kiel, following the method described in *Heuser et al*. [2002] and *Tang et al*. [2008]. Aliquots of 0.1 mg were dissolved in 2.2 N ultrapure HCl, dried down and redissolved in 2.2 N HCl with a Ca concentration of 160 ng/µL. The sample solutions were mixed with a $^{43}Ca/^{48}Ca$ double spike (with the spike contributing about 90 % of ^{48}Ca) and about 300 ng of each sample-spike mixture was loaded with $TaCl_5$ activator on an outgassed zone-refined Re filament. Measurements were made on single filaments at a temperature of about 1500°C and a typical ^{40}Ca signal intensity of 50 pA (5 V). Data acquisition was performed in dynamic mode. The acquired data were fractionation corrected online to the spike $^{43}Ca/^{48}Ca$ ratio of 0.748429 [*Gussone*, 2003] using the exponential fractionation law. The double spike correction was carried out with the iterative algorithm described by *Heuser et al*. [2002].

[13] The isotope values of Ca are reported as $\delta^{44/40}Ca$ values relative to the NIST standard SRM915a, where $\delta^{44/40}Ca = [(^{44}Ca/^{40}Ca)_{sample}/(^{44}Ca/^{40}Ca)_{SRM915a} - 1] \times 1000$. The samples are normalized to the mean $^{44}Ca/^{40}Ca$ of four SRM915a analyses, run on the same turret. The sample precision is given as two times the standard error of the mean determined (2 err) by repeated measurements of the sample stock solutions. All samples were measured at least twice. The average 2 err is 0.12‰. The spike corrected mean $^{44}Ca/^{40}Ca$ of NIST SRM915a was 0.021185(3) (standard deviation, $n = 17$). Total Ca blanks for the isotope analyses were less than 1%.

3. Results

[14] The morphologies and succession of foliate layers and chalky substance in the umbo of the three specimens vary considerably (Figure 3), but isotopic and element profiles show strong similarities in trends and absolute values (Figure 4). The carbon and oxygen isotope values of the oysters (including the data from *Ullmann et al*. [2010]) vary between −1.9 and +1.0‰ and between −3.0 and +1.3‰, respectively (see supporting information). The data sets for specimen vl of the present study and of *Ullmann et al*. [2010] are in a good agreement (Figure 4). All four annual cycles of the years 2004–2007 reported in the previous study are represented here at about half of the former spatial resolution. The reduced resolution is due to the larger sample sizes necessary, and because of a less favorable section through the umbo of the shell (Figure 2; see sections 2.1 and 2.2 for details). Oxygen isotope profiles through specimens 8l and 1l indicate 5 growth seasons (2003–2007) (Figure 4).

[15] Where sufficient material was available for submonthly sample resolution, minimum $\delta^{18}O$ values between the analyzed specimens agree within 0.4‰ for all growth seasons (Figure 4). Larger disagreements for annual maxima and average $\delta^{18}O$ values are due to shell morphology and differential shell growth (Figure 4).

[16] Carbon isotope values show systematic variations in all three specimens and average $\delta^{13}C$ values of the specimens of −1.27 to −1.17‰ agree within 0.1‰. An increase of the $\delta^{13}C$ values at the beginning of each growth season is indicated, but annual trends differ in details.

[17] Trace element data are given in Figure 4 and the online supporting information. All the samples are composed of low-Mg-calcite with Mg/Ca ratios varying between 2.5 and 14.6 mmol/mol (Figures 4c, 4h, and 4m). The median Mg/Ca ratios for the foliate layers—excluding the first growth season—range from 3.7 to 4.1 mmol/mol (Figure 5). Mg/Ca ratios of the foliate layers are

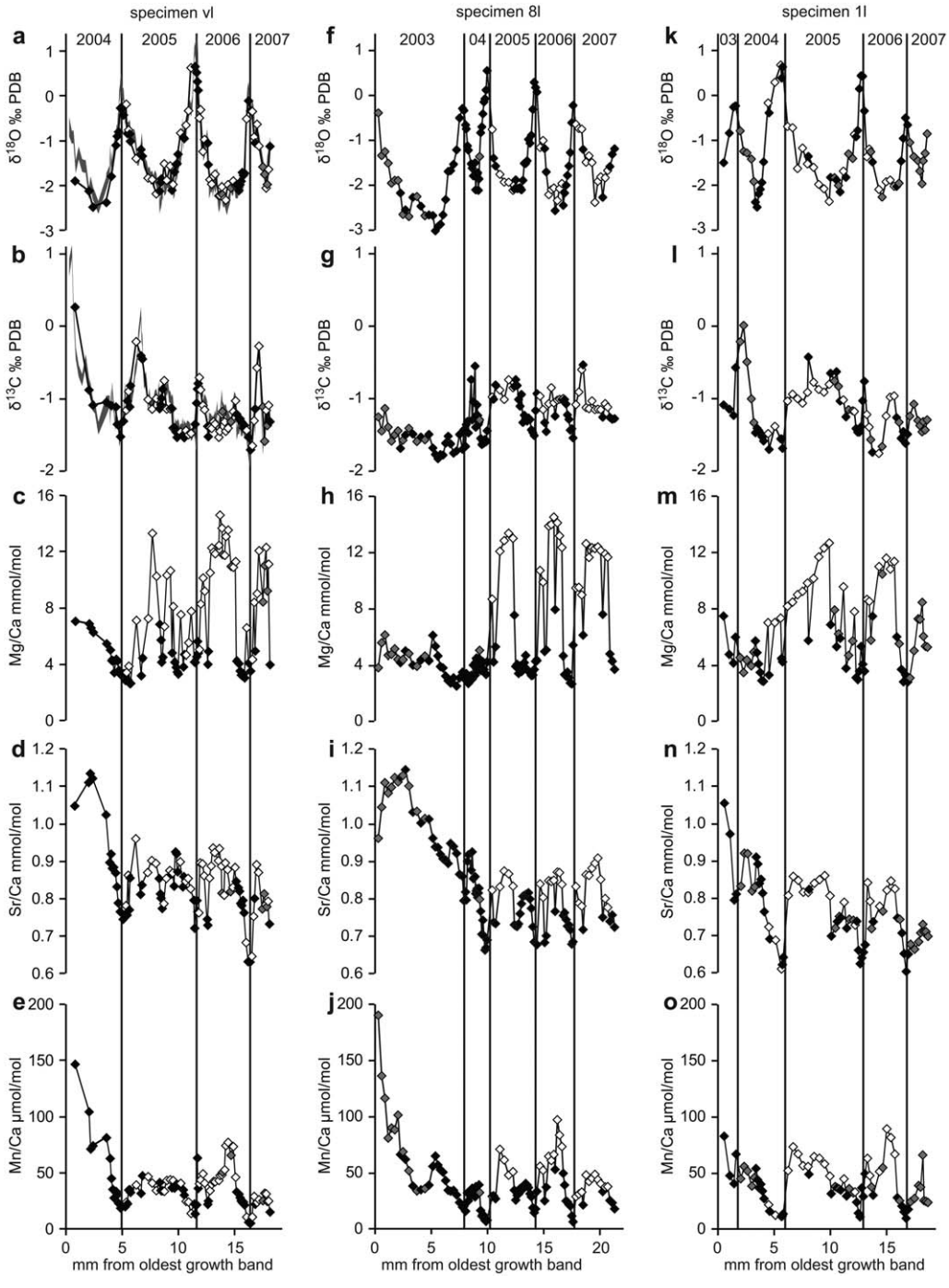

Figure 4. Geochemical results for shell carbonate plotted against distance from the earliest growth bands. Sample positions of specimen vl from this study are correlated with the previous study of *Ullmann et al*. [2010] by matching the growth bands. (a–e) Specimen vl; (f–j) specimen 8l; and (k–o) specimen 1l. White diamonds: chalky substance; gray diamonds: mixed samples containing material from foliate layers and chalky substance; black samples: foliate layers. Gray bands in Figures 4a and 4b represent isotope data presented in *Ullmann et al*. [2010].

not correlated with $\delta^{18}O$ (Figure 6a). The Mg/Ca ratios in the chalky substance, compared to the foliate layers, are enriched in Mg more than twofold with median Mg/Ca ratios of 9.4–12.3 mmol/mol (Figure 5a). In addition, Mg/Ca ratios in the chalky substance show a seasonal pattern with the highest ratios in the warm season (Figures 4c, 4h, and 4m). This seasonal pattern is expressed in a

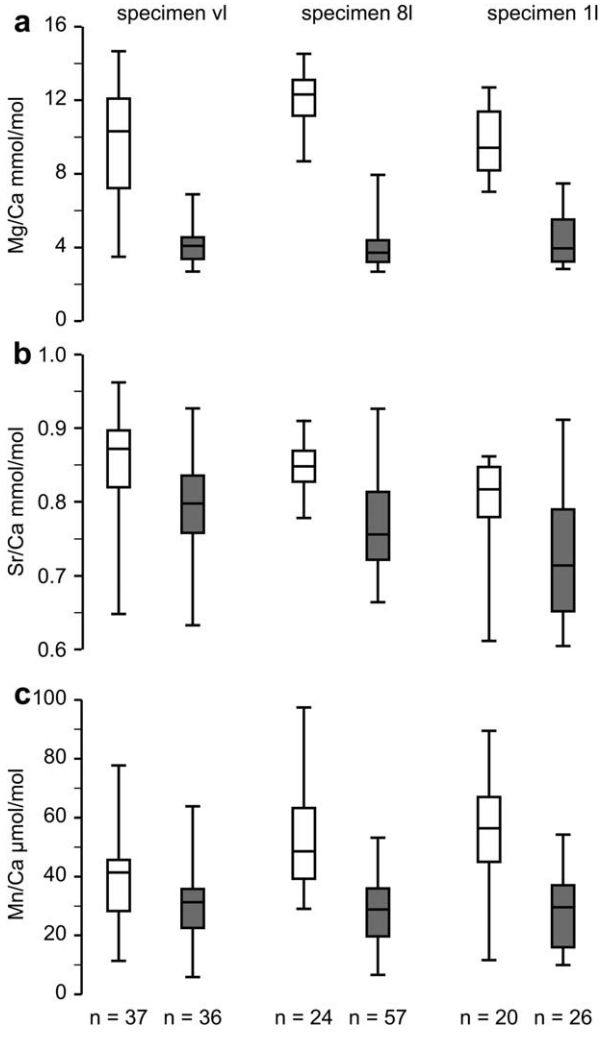

Figure 5. Box plots of element ratios in foliate layers and chalky substance of the three specimens. The boxes represent the second and third quartile with the median value as a black line and the whiskers show the full range of observed ratios.

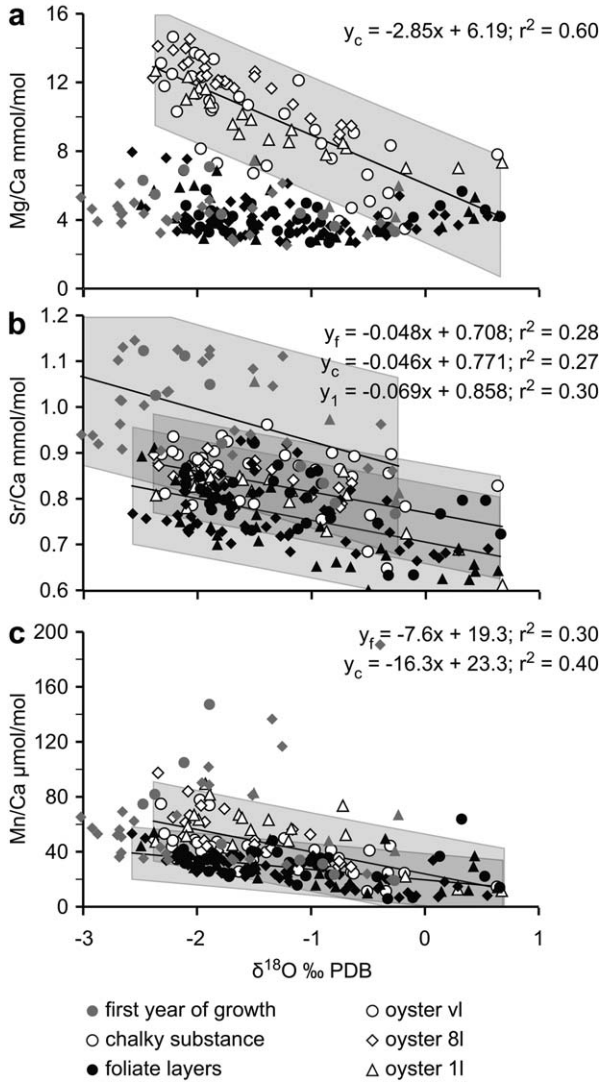

Figure 6. Element ratios plotted against oxygen isotope values. Trend lines of correlations with $r^2 > 0.2$ are plotted with 95% confidence intervals as gray bands.

strong, negative, correlation of Mg/Ca ratios of all specimens with $\delta^{18}O$ values of the form $Mg/Ca_{chalky} = -2.85 \pm 0.52 \times \delta^{18}O + 6.19 \pm 0.83$ ($r^2 = 0.60$, Figure 6a).

[18] The Sr/Ca ratios of the specimens range from 0.60 to 1.14 mmol/mol (Figures 4d, 4i, and 4n). For all specimens, the highest Sr/Ca ratios are measured in the samples of the first growth season. A seasonal pattern of Sr/Ca ratios can be recognized but is not very pronounced (Figures 4d, 4i, and 4n) and weak, negative, correlations of Sr/Ca ratios with $\delta^{18}O$ values exist for the samples from the respective first growth seasons ($r^2 = 0.30$), foliate layers ($r^2 = 0.28$), and chalky substance ($r^2 = 0.27$) (Figure 6b). The equations with 95% confidence intervals for these correlations are $Sr/Ca_{1st\ season} = -0.0069 \pm 0.0035 \times \delta^{18}O + 0.858 \pm 0.068$; $Sr/Ca_{foliate} = -0.0048 \pm 0.0015 \times \delta^{18}O + 0.708 \pm 0.021$; and $Sr/Ca_{chalky} = -0.0046 \pm 0.0015 \times \delta^{18}O + 0.771 \pm 0.026$. The median Sr/Ca ratios of the chalky substance of 0.82–0.87 mmol/mol are similar for the three specimens (Figure 5b). Also the median Sr/Ca ratios of the foliate layers of 0.71–0.80 mmol/mol (excluding data from the first growth season) are similar but 9–13% lower than the respective values of the chalky substance (Figure 5b).

[19] The Mn/Ca ratios exhibit the highest relative variability of the three element ratios and vary from 6 to 190 µmol/mol (Figures 4e, 4j, and 4o). Analogous to the Sr/Ca ratios, the Mn/Ca ratios decrease strongly from the highest ratios measured for the shell in the first growth season. A seasonal

pattern with higher Mn/Ca ratios in the warm season is observed. Like Sr/Ca ratios, Mn/Ca ratios of foliate layers and chalky substance correlate negatively with $\delta^{18}O$ values ($r^2 = 0.30$ and 0.40, respectively; Figure 6c). As for Sr/Ca and Mg/Ca, median Mn/Ca ratios of the respective shell materials of the three specimens are similar, but median Mn/Ca ratios of the chalky substance are ~20–50% higher than median Mn/Ca ratios of the foliate layers (Figure 5c).

[20] The calcium isotopic composition of specimen vl is constant within analytical uncertainty (Figure 7), precluding a visible ontogenic trend. No correlation with the oxygen isotope ratios is found and the chalky substance ($\delta^{44/40}Ca = 0.66 \pm 0.04$‰) and foliate layers ($\delta^{44/40}Ca = 0.70 \pm 0.07$‰) have indistinguishable compositions.

4. Discussion

4.1. Carbon and Oxygen Isotopes

[21] The assumption of *Ullmann et al*. [2010] that *C. gigas* records a high fidelity $\delta^{18}O$ signature is supported by the reproducibility of the signature within the same specimen (Figure 4a) and in other specimens (Figures 4f and 4k). The excellent agreement between the isotope profiles through two sections of the umbo of specimen vl (Figures 4a and 4b) indicates that the carbon and oxygen isotope ratios of coeval growth bands are uniform. The slightly smaller amplitude for the reproduced profile can be explained by time averaging [*Goodwin et al*., 2003], generated by the larger samples compared to the sample amounts that were taken for carbon and oxygen isotope analyses in *Ullmann et al*. [2010].

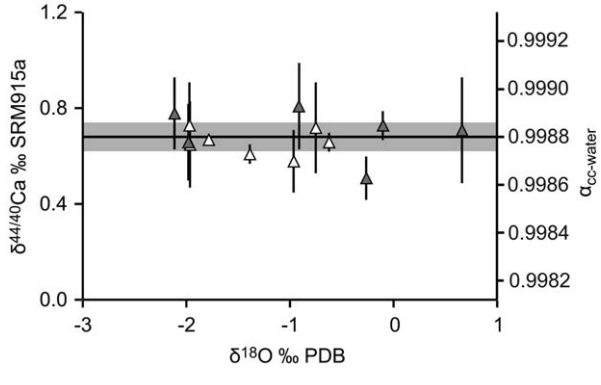

Figure 7. Ca isotope values and respective $^{44}Ca/^{40}Ca$ fractionation factor ($\alpha_{cc\text{-}water}$) for shell calcite of *C. gigas*. White triangles: chalky substance and gray triangles: foliate layers. Black line: mean value with 2 err uncertainty.

[22] The generally low variability of the $\delta^{13}C$ values within the specimens of ~0.7‰ (2 sd) and the very good agreement between the average values of different specimens attest that vital effects in *C. gigas* are not expressed as large isotope fluctuations and biases differing between individual specimens. Moreover, a correlation between oxygen and carbon isotope ratios, suggesting kinetic isotope fractionation during incorporation of the carbonate ion into the crystal lattice [e.g., *Parkinson et al*., 2005, for brachiopods], is not found here. These findings suggest that *C. gigas* records the $\delta^{13}C$ signature of the water DIC without major bias. In the absence of direct measurements of $\delta^{13}C_{DIC}$ in the List Basin, this hypothesis cannot be further strengthened. It remains unclear, if increasing $\delta^{13}C$ values in our shell material, coinciding with the timing of phytoplankton blooms in the late spring [*van Beusekom et al*., 2009], are related to changes in the ambient DIC [*Wang et al*., 1995; *Goodwin et al*., 2013] or are controlled by metabolic processes.

4.2. Ca Isotopes

[23] The lack of a correlation with temperature or seasonal effects in *C. gigas*, expressed by the uniformity of the calcium isotope ratios (Figure 7), is in agreement with an apparently small temperature dependence of Ca isotope fractionation in other biogenic carbonates [*Steuber and Buhl*, 2006; *Farkaš et al*., 2007; but see *Immenhauser et al*., 2005]. The $\delta^{44/40}Ca$ of open ocean seawater was found to be globally homogeneous at a value of 1.88 ± 0.04‰ versus SRM915a [*Hippler et al*., 2003]. This is also true for most marginal seas, including the North Sea near Sylt and the Baltic Sea [*Heinemann et al*., 2008], the Mediterranean Sea [*Böhm et al*., 2006], and the Red Sea [*Kisakürek et al*., 2011]. The mean of the measured values of $\delta^{44/40}Ca = 0.68 \pm 0.04$‰ versus SRM915a can therefore be used to define a fractionation factor $\alpha_{cc\text{-}water}$ between the shell calcite and sea water (Figure 7). The fractionation factor determined for *C. gigas* from the $\delta^{44/40}Ca$ value of seawater and the average $\delta^{44/40}Ca$ value of the shell calcite is $\alpha_{cc\text{-}water} = 0.99880 \pm 0.00006$. This result is in good agreement with the fractionation factor calculated for a calcite shell layer of *Mytilus edulis* ($\alpha_{cc\text{-}water} = 0.9989$) collected from the same region [*Heinemann et al*., 2008]. It further agrees with the average fractionation factor for marine biogenic calcite at ~15°C from *Gussone et al*. [2005], $\alpha_{cc\text{-}water} = 0.9989$. The fractionation factor for *C. gigas* for the List Basin is significantly

higher than the value of 0.9985 found by *Steuber and Buhl* [2006] for modern oysters from the North Sea. The differing fractionation factor found by *Steuber and Buhl* [2006] might be due to more pronounced freshwater influx changing the $\delta^{44/40}$Ca ratio of the ambient water [*Heinemann et al*., 2008; *Holmden et al*., 2012]. Also comparatively high Mn/Ca ratios of the specimens of *Steuber and Buhl* [2006] point to a freshwater influenced setting [*Almeida et al*., 1998].

4.3. Element Ratios

[24] Contrasting to the isotopic signatures of the oyster specimens, element ratios in the shell materials differ significantly between chalky substance and foliate layers (Figures 4–6). For Sr/Ca and Mn/Ca, the highest ratios are observed in the first growth season. The high Sr/Ca and Mn/Ca ratios recorded by specimen vl in 2004 are not observed in specimens 8l and 11, for which 2004 represents the second growth season. This difference evidences that the enrichments of the respective first growth seasons are related to metabolic processes and not to an environmental control. The differing incorporation behavior of Mg into foliate layers and chalky substance strengthens this hypothesis. For the interpretation of element ratios, the samples from the first growth season are therefore treated separately.

[25] Mg/Ca ratios for oysters published so far range from 5.5 to 27 mmol/mol [*Lerman*, 1965; *Ohde and Kitano*, 1984; *Almeida et al*., 1998]. The average values of our specimens ranging from 5.8 to 6.8 mmol/mol fall into this range, but most of the samples from foliate layers show lower ratios (Figures 4c, 4h, 4m, 5a, and 6a). Salinities are too high and stable (Figure 1c) [*van Beusekom et al*., 2008; *Ullmann et al*., 2010] to result in a potential major effect on Mg/Ca ratios, either by changes in water composition [*Dodd and Crisp*, 1982; *Carré et al*., 2006], or salinity-related changes in element fractionation [*Eisma et al*., 1976]. The oxygen isotope values of the investigated oyster vary strongly throughout the year, following primarily the temperature of the ambient water (see *Ullmann et al*. [2010] for detailed discussion). The strong, negative, correlation of Mg/Ca ratios with δ^{18}O values of the chalky substance ($r^2 = 0.60$) indicates that Mn/Ca ratios is controlled largely by temperature, pointing to Mg/Ca ratios in the chalky substance of *C. gigas* as a promising proxy for temperatures. Mg/Ca temperature proxies using bivalve calcite [e.g., *Vander Putten et al*., 2000; *Ford et al*., 2010; *Heinemann et al*., 2011; *Schöne et al*, 2011; *Freitas et al*., 2012] can be interesting for environmental reconstructions, if the covariations of Mg/Ca with temperature are very strong. Further studies, including δ^{18}O measurements of ambient water and using environmental data with better time resolution might show, if the chalky substance of *C. gigas* is suitable for such reconstructions.

[26] The Mg/Ca ratios of the foliate layers of *C. gigas* do not show a strong covariance with δ^{18}O values ($r^2 = 0.05$) and their averages of 4.1–4.3 mmol/mol (excluding the first growth season) agree within 5% for the three investigated specimens. Mg/Ca ratios of foliate layers might thus be used to estimate seawater Mg/Ca ratios. Together with a seawater Mg/Ca ratio of 5.2 mol/mol [*de Villiers and Nelson*, 1999], our observed average Mg/Ca ratios for the foliate layers of the three specimens translate into a Mg distribution coefficient of 0.00080 ± 0.00003 (2 err, $n = 3$) for *C. gigas* in the List Basin. The internal variability of each specimen, however, is on the order of 50% (2 rsd), necessitating the measurement of numerous or large samples to derive a reliable mean value.

[27] The average Sr/Ca ratio of our oyster material of 0.82 mmol/mol ($n = 271$) compares well with data published for oyster shell material of *Malleus albus* (0.81 mmol/mol, $n = 1$), *C. gigas* (0.83 mmol/mol, $n = 268$), *Crassostrea virginica* (0.86 mmol/mol, $n = 10$), and *Saxostrea gigas* (1.06 mmol/mol, $n = 1$) [*Lerman*, 1965; *Ohde and Kitano*, 1984; *Almeida et al*., 1998]. Weak negative correlations of Sr/Ca ratios with oxygen isotope values (Figure 6b) indicate that seasonal effects may play a role in the incorporation of Sr into the shell of *C. gigas*. Together with a seawater Sr/Ca ratio of 8.54 mmol/mol [*de Villiers*, 1999], and assuming an average δ^{18}O value of the ambient water in the List Basin of −1.4‰ SMOW [*Ullmann et al*., 2010], calibrations for foliate layers and chalky substance can be derived from these empirical covariations. The resulting equations are $D_{Sr\ foliate} = 0.0907 \pm 0.0027 - 0.0056 \pm 0.0017 \times (\delta^{18}O_{calcite} - \delta^{18}O_{water})$ for foliate layers and $D_{Sr\ chalky} = 0.0978 \pm 0.0033 - 0.0053 \pm 0.0020 \times (\delta^{18}O_{calcite} - \delta^{18}O_{water})$ for the chalky substance of *C. gigas*. The above distribution coefficients are consistently lower than for *Pinna nobilis* [*Richardson et al*., 2004], *Pecten maximus* [*Lorrain et al*., 2005; *Freitas et al*., 2006], and brachiopods living in water depths of less than 100 m [*Brand et al*., 2003], a relationship that is also observed for Early Jurassic specimens [e.g., *Korte and Hesselbo*, 2011]. The Sr distribution coefficients for *C. gigas*

in the List Basin might therefore serve as approximations for the derivation of past seawater Sr/Ca ratios using ostreoid materials.

[28] The Mn/Ca ratios in our oyster specimens, ranging from 6 to 190 μmol/mol ($n = 271$), are in very good agreement with the values reported for modern Portuguese oysters of 12–93 μmol/mol [*Almeida et al*., 1998], considering that only 6 values > 100 μmol/mol were measured in our samples. Among other features, peak Mn/Ca ratios in the second half of 2006 and comparatively low Mn/Ca ratios in 2007 are common to all three specimens (Figures 4e, 4j, and 4o), indicating that these systematic trends may be partially controlled by changing Mn/Ca ratios of ambient water. Such an environmental control on Mn/Ca ratios has also been observed for *Pecten maximus* [*Freitas et al*., 2006]. The high Mn/Ca ratios of the oyster's first growth season (Figures 4e, 4j, 4o, and 5) and the differing Mn incorporation trends of foliate layers and chalky substance demonstrate that an additional biological control on Mn uptake, as also invoked by *Freitas et al*. [2006], is an important factor.

[29] Mn concentrations of biogenic carbonates are often taken as quality markers for fossil preservation [e.g., *Prokoph et al*., 2008; *Korte et al*., 2009]. Mn/Ca ratios of up to ~100 μmol/mol [*Almeida et al*., 1998; *Steuber and Buhl* 2006], as well as Mn/Ca ratios of up to 450 μmol/mol in *Mytilus edulis* [*Vander Putten et al*., 2000], are evidence for potentially elevated Mn/Ca ratios in calcite shells that are not necessarily generated by post-depositional alteration (see also *Korte and Hesselbo* [2011]). Also, significant negative correlations of Mn concentrations with $\delta^{18}O$ values are taken as markers for diagenetic trends [e.g., *Brand and Veizer*, 1981]. The negative correlations of Mn/Ca ratios with $\delta^{18}O$ values found in modern *C. gigas* shells underline that the interpretation of such empirical covariations in fossil materials may not always be straight forward. In studies on fossil materials, additional proxies for alteration that are independent of Mn concentrations should be employed to address such ambiguities.

5. Conclusions

[30] C and O isotope trends and average values in all three specimens of modern *C. gigas* are similar, indicating that disequilibrium isotope fractionation plays a minor role during shell formation.

[31] Ca isotope ratios are constant within analytical precision throughout the lifespan of a single oyster and a fraction factor for $^{44}Ca/^{40}Ca$ of $\alpha_{cc\text{-}water} = 0.99880 \pm 0.00006$ is derived. The isotopic uniformity of Ca suggests that palaeoseawater calcium isotopic compositions can be deduced from shells of *C. gigas* (and other oysters).

[32] Element/Ca ratios show metabolically controlled enrichments in the first growth season and are lower in the foliate layers than in the chalky substance. Significant correlations of element/Ca ratios with oxygen isotope ratios and $r^2 > 0.20$ are observed for all element ratios apart from Mg/Ca ratios in the foliate layers. An Mg distribution coefficient of $D_{Mg} = 0.00080 \pm 0.00003$ is found for the foliate layers of *C. gigas*. The covariation of Mg/Ca ratios in the chalky substance of *C. gigas* with $Mg/Ca_{chalky} = -2.85 \pm 0.52 \times \delta^{18}O_{calcite} + 6.19 \pm 0.83$ can mainly be explained by temperature dependent element incorporation. Empirical Sr distribution coefficients are $D_{Sr\ foliate} = 0.0907 \pm 0.0027 - 0.0056 \pm 0.0017 \times (\delta^{18}O_{calcite} - \delta^{18}O_{water})$ for foliate layers and $D_{Sr\ chalky} = 0.0978 \pm 0.0033 - 0.0053 \pm 0.0020 \times (\delta^{18}O_{calcite} - \delta^{18}O_{water})$ for the chalky substance. Trends in Mn/Ca ratios are likely controlled by a combination of metabolic factors and the changing Mn/Ca ratio of the ambient water.

Acknowledgments

[33] The authors acknowledge the editor Louis Derry, an anonymous associate editor, and two anonymous reviewers for comments and suggestions that helped to greatly improve the manuscript. The authors acknowledge Karsten Reise for taking the samples in the field, Cees-Jan DeHoog for ICP-MS measurements at the University of Oxford, Bo Petersen for carbon and oxygen isotope analyses at the University of Copenhagen, and Stephen Hesselbo for providing accommodation and assistance during the work stay in Oxford. The project was funded by the Center for International Cooperation, Freie Universität Berlin (travel grant for CVU) and by the DFG (project Ei 272/13). We thank Anton Eisenhauer and Folkmar Hauff (GEOMAR) for help and support for the TIMS analyses at Geomar.

References

Almeida, M. J., J. Machado, G. Moura, M. Azevedo, and J. Coimbra (1998), Temporal and local variations in biochemical composition of *Crassostrea gigas* shells, *J. Sea Res.*, *40*, 233–249.

Ayoub-Hannaa, W., and F. T. Fürsich (2011), Functional morphology and taphonomy of Cenomanian (Cretaceous) oysters from the eastern Sinai Peninsula, Egypt, *Palaeobio. Paleoenv.*, *91*, 197–214.

Blättler, C. L., G. M. Henderson, and H. C. Jenkyns (2012), Explaining the Phanerozoic Ca isotope history of seawater, *Geology*, *40*, 843–846, doi:10.1130/G33191.1.

Böhm, F., N. Gussone, A. Eisenhauer, W.-C. Dullo, S. Reynaud, and A. Paytan (2006), Calcium isotope fractionation in modern scleractinian corals, *Geochim. Cosmochim. Acta*, *70*, 4452–4462.

Brand, U., and J. Veizer (1981), Chemical diagenesis of a multicomponent carbonate system—2: Stable isotopes, *J. Sediment. Petrol.*, *51*(3), 987–997.

Brand, U., A. Logan, N. Hiller, and J. Richardson (2003), Geochemistry of modern brachiopods: Applications and implications for oceanography and paleoceanography, *Chem. Geol.*, *198*, 305–334.

Buchardt, B. (1978), Oxygen isotope palaeotemperatures from the Tertiary period in the North Sea area, *Nature*, *275*, 121–123.

Carré, M., I. Bentaleb, O. Bruguier, E. Ordinola, N. T. Barrett, and M. Fontugne (2006), Calcification rate influence on trace element concentrations in aragonitic bivalve shells: Evidences and mechanisms, *Geochim. Cosmochim. Acta*, *70*, 4906–4920.

Carriker, M. R., and R. E. Palmer (1979), Ultrastructural morphogenesis of prodissoconch and early dissoconch valves of the Oyster Crassostrea virginica, *Proc. Natl. Shellfish. Assoc.*, *69*, 103–128.

Carriker, M. R., R. E. Palmer, and R. S. Prezant (1980), Functional ultramorphology of the dissoconch valves of the Oyster Crassostrea virginica, *Proc. Natl. Shellfish. Assoc.*, *70*, 139–183.

Chinzei, K. (1986), Shell structure, growth, and functional morphology of an elongate cretaceous oyster, *Palaeontology*, *29*(1), 139–154.

Dauphin, Y., A. B. Ball, H. Castillo-Michel, C. Chevallard, J.-P. Cuif, B. Farre, S. Pouvreau, and M. Salomé (2013), *In situ* distribution and characterization of the organic content of the oyster shell *Crassostrea gigas* (Mollusca, Bivalvia), *Micron*, *44*, 373–383.

de Villiers, S. (1999), Seawater strontium and Sr/Ca variability in the Atlantic and Pacific oceans, *Earth Planet. Sci. Lett.*, *171*, 623–634.

de Villiers, S., and B. K. Nelson (1999), Detection of low-temperature hydrothermal fluxes by seawater Mg and Ca anomalies, *Science*, *285*, 721–723.

Dodd, J. R., and E. L. Crisp (1982), Non-linear variation with salinity of Sr/Ca and Mg/Ca ratios in water and aragonitic bivalve shells and implications for paleosalinity studies, *Palaeogeogr. Palaeoclimatol. Palaeoecol.*, *38*, 45–56.

Eisma, D., W. G. Mook, and H. A. Das, (1976), Shell characteristics, isotopic composition and trace-element contents of some euryhaline molluscs as indicators of salinity, *Palaeogeogr. Palaeoclimatol. Palaeoecol.*, *19*, 39–62.

Farkaš, J., F. Böhm, K. Wallmann, J. Blenkinsop, A. Eisenhauer, R. van Geldern, A. Munnecke, S. Voigt, and J. Veizer (2007), Calcium isotope record of Phanerozoic oceans: Implications for chemical evolution of seawater and its causative mechanisms, *Geochim. Cosmochim. Acta*, *71*, 5117–5134.

Ferguson, J. E., G. M. Henderson, M. Kucera, and R. E. M. Rickaby (2008), Systematic change of foraminiferal Mg/Ca ratios across a strong salinity gradient, *Earth Planet. Sci. Lett.*, *265*, 153–166.

Ford, H. L., S. A. Schellenberg, B. J. Becker, D. L. Deutschman, K. A. Dyck, and P. L. Koch (2010), Evaluating the skeletal chemistry of *Mytilus californianus* as a temperature proxy: Effects of microenvironment and ontogeny, *Paleoceanography*, *25*, PA1203, doi:10.1029/2008PA001677.

Freitas, P. S., L. J. Clarke, H. Kennedy, C. A. Richardson, and F. Abrantes (2006), Environmental and biological controls on elemental (Mg/Ca, Sr/Ca and Mn/Ca) ratios in shells of the king scallop *Pecten maximus*, *Geochim. Cosmochim. Acta*, *70*, 5119–5133.

Freitas, P. S., L. J. Clarke, H. Kennedy, and C. A. Richardson (2012), The potential of combined Mg/Ca and $\delta^{18}O$ measurements within the shell of the bivalve *Pecten maximus* to estimate seawater $\delta^{18}O$ composition, *Chem. Geol.*, *291*, 286–293.

Goodwin, D. H., B. R. Schöne, and D. L. Dettman (2003), Resolution and fidelity of oxygen isotopes as paleotemperature proxies in bivalve mollusk shells: Models and observations, *Palaios*, *18*, 110–125.

Goodwin, D. H., D. P. Gillikin, and P. D. Roopnarine (2013), Preliminary evaluation of potential stable isotope and trace element productivity proxies in the oyster *Crassostrea gigas*, *Palaeogeogr. Palaeoclimatol. Palaeoecol.*, *373*, 88–97.

Gussone, N. (2003), Calcium isotopes in calcium carbonates: Calibration and application, PhD thesis, p. 134, Christian-Albrechts-Univ., Kiel.

Gussone, N., F. Böhm, A. Eisenhauer, M. Dietzel, A. Heuser, B. M. A. Teichert, J. Reitner, G. Worheide, and W.-C. Dullo (2005), Calcium isotope fractionation in calcite and aragonite, *Geochim. Cosmochim. Acta*, *69*, 4485–4494.

Heinemann, A., J. Fietzke, A. Eisenhauer, and K. Zumholz (2008), Modification of Ca isotope and trace metal composition of the major matrices involved in shell formation of *Mytilus edulis*, *Geochem. Geophys. Geosyst.*, *9*, Q01006, doi:10.1029/2007GC001777.

Heinemann, A., C. Hiebenthal, J. Fietzke, A. Eisenhauer, and M. Wahl (2011), Disentangling the biological and environmental control of *M. edulis* shell chemistry, *Geochem. Geophys. Geosyst.*, *12*, Q03009, doi:10.1029/2010GC003340.

Heuser, A., A. Eisenhauer, N. Gussone, B. Bock, B. T. Hansen, and T. F. Nägler (2002), Measurement of calcium isotopes ($\delta^{44}Ca$) using a multicollector TIMS technique, *Int. J. Mass Spectrom.*, *220*, 385–397.

Hippler, D., A.-D. Schmitt, N. Gussone, A. Heuser, P. Stille, A. Eisenhauer, and T. F. Nägler (2003), Calcium isotopic composition of various reference materials and seawater, *Geostand. Newsl.*, *27*(1), 13–19.

Holmden, C., D. A. Papanastassiou, P. Blanchon, and S. Evans (2012), $\delta^{44/40}Ca$ variability in shallow water carbonates and the impact of submarine groundwater discharge on Ca-cycling in marine environments, *Geochim. Cosmochim. Acta*, *83*, 179–194.

Imai, N., S. Terashima, S. Itoh, and A. Ando (1996), 1996 compilation of analytical data on nine GSJ geochemical reference samples, ''Sedimentary rock series,'' *Geostand. Newsl.*, *20*(2), 165–216.

Immenhauser, A., T. F. Nägler, T. Steuber, and D. Hippler (2005), A critical assessment of mollusk $^{18}O/^{16}O$, Mg/Ca and $^{44}Ca/^{40}Ca$ ratios as proxies for Cretaceous seawater temperature seasonality, *Palaeogeogr. Palaeoclimatol. Palaeoecol.*, *215*, 221–237.

Kisakürek, B., A. Eisenhauer, F. Böhm, E. C. Hathorne, and J. Erez (2011), Controls on calcium isotope fractionation in cultured planktic foraminifera, *Globigerinoides ruber* and Globigerinella siphonifera, *Geochim. Cosmochim. Acta*, 75, 427–443.

Klein, R. T., K. C. Lohmann, and C. W. Thayer (1996), Sr/Ca and $^{13}C/^{12}C$ ratios in skeletal calcite of *Mytilus trossulus*: Covariation with metabolic rate, salinity, and carbon isotopic composition of seawater, *Geochim. Cosmochim. Acta*, *60*(21), 4207–4221.

Komatsu, T., K. Chinzei, M. S. Zakhera, and H. Matsuoka (2002), Jurassic soft-bottom oyster *Crassostrea* from Japan, *Paleontology*, *45*(6), 1037–1048.

Korte, C., and S. P. Hesselbo (2011), Shallow marine carbon and oxygen isotope and elemental records indicate icehouse-greenhouse cycles during the Early Jurassic, *Paleoceanography*, *26*, PA4219, doi:10.1029/2011PA002160.

Korte, C., S. P. Hesselbo, H. C. Jenkyns, R. E. M. Rickaby, and C. Spötl (2009), Palaeoenvironmental significance of carbon- and oxygen-isotope stratigraphy of marine Triassic-Jurassic boundary sections in SW Britain, *J. Geol. Soc.*, *166*, 431–445.

Leal, J. C. M., S. Dubois, F. Orvain, R. Galois, J.-L. Blin, M. Ropert, M.-P. Bataillé, A. Ourry, and S. Lefebvre (2008), Stable isotopes ($\delta^{13}C$, $\delta^{15}N$) and modelling as tools to estimate the trophic ecology of cultivated oysters in two contrasting environments, *Mar. Biol.*, *153*, 673–688.

Lee, S. W., and C. S. Choi (2007), The correlation between organic matrices and biominerals (myostracal prism and folia) of the adult oyster shell, C*rassostrea gigas*, *Micron*, *38*, 58–64.

Lee, S. W., S. M. Hong, and C. S. Choi (2006), Characteristics of calcification processes in embryos and larvae of the pacific oyster, *Crassostrea gigas*, *Bull. Mar. Sci.*, *78*(2), 309–317.

Lee, S.-W., Y.-N. Jang, K.-W. Ryu, S.-C. Chae, and Y.-H. Lee (2011), Mechanical characteristics and morphological effect of complex crossed structure in biomaterials: Fracture mechanics and microstructure of chalky layer in oyster shell, *Micron*, *42*, 60–70.

Lerman, A. (1965), Paleoecological problems of Mg and Sr in biogenic calcites in light of recent thermodynamic data, *Geochim. Cosmochim. Acta*, *29*, 977–1002.

Lorrain, A., D. P. Gillikin, Y.-M. Paulet, L. Chauvaud, A. Le Mercier, J. Navez, and L. André (2005), Strong kinetic effects on Sr/Ca ratios in the calcitic bivalve *Pecten maximus*, *Geology*, *33*(12), 965–968.

MacDonald, J., A. Freer, and M. Cusack (2009), Alignment of crystallographic c-axis throughout the four distinct microstructural layers of the oyster *Crassostrea gigas*, *Cryst. Growth Design*, *10*, 1243–1246.

Marie, B., I. Zanella-Cléon, N. Guichard, M. Becchi, and F. Marin (2011), Novel proteins from the calcifying shell matrix of the Pacific oyster *Crassostrea gigas*, *Mar. Biotechnol.*, *13*, 1159–1168.

Miyawaki, M. (1954), Notes on the shell structure of the oyster, Gryphea (Ostrea) gigas from the Akkeshi Lake, *J. Fac. Sci. Hokkaido Univ. Ser. VI, Zool.*, *12*, 116–119.

Ohde, S., and Y. Kitano (1984), Coprecipitation of strontium with marine Ca-Mg carbonates, *Geochem. J.*, *18*, 143–146.

Parkinson, D., G. B. Curry, M. Cusack, and A. E. Fallick (2005), Shell structure, patterns and trends of oxygen and stable isotopes in modern brachiopod shells, *Chem. Geol.*, *219*, 193–235.

Pauley, G. B., B. Van Der Raay, and D. Troutt (1988), Species profiles: Life histories and environmental requirements of coastal fishes and invertebrates (Pacific Northwest)—Pacific oyster, U.S. Fish Wildl. Serv. Biol. Rep. 82(11.85), U.S. Army Corps of Engineers, TR EL-82.4., Research and Development, National Wetlands Research Center, Washington, DC, 20240, 28 pp.

Prokoph, A., G. A. Shields, and J. Veizer (2008), Compilation and time-series analysis of marine carbonate $\delta^{18}O$, $\delta^{13}C$, $^{87}Sr/^{86}Sr$ and $\delta^{34}S$ database through Earth history, *Earth Sci. Rev.*, *87*, 113–133.

Quayle, D.B. (1969), Pacific oyster culture in British Columbia, *Fish. Res. Board Can. Bull.*, *169*, 192 pp.

Richardson, C. A., M. Peharda, H. Kennedy, P. Kennedy, and V. Onofri (2004), Age, growth rate and season of recruitment of *Pinna nobilis* (L) in the Croatian Adriatic determined from Mg:Ca and Sr:Ca shell profiles, *J. Exp. Mar. Biol. Ecol.*, *299*, 1–16.

Schöne, B. R., Z. Zhang, P. Radermacher, J. Thébault, D. E. Jacob, E. V. Nunn, and A.-F. Maurer (2011), Sr/Ca and Mg/Ca ratios of ontogenetically old, long-lived bivalve shells (*Arctica islandica*) and their function as paleotemperature proxies, *Palaeogeogr. Palaeoclimatol. Palaeoecol.*, *302*, 52–64.

Steuber, T., and D. Buhl (2006), Calcium-isotope fractionation in selected modern and ancient marine carbonates, *Geochim. Cosmochim. Acta*, *70*, 5507–5521.

Steuber, T., and J. Veizer (2002), Phanerozoic record of plate tectonic control of seawater chemistry and carbonate sedimentation, *Geology*, *30*, 1123–1126.

Tang, J., M. Dietzel, F. Böhm, S. J. Köhler, and A. Eisenhauer (2008), Sr^{2+}/Ca^{2+} and $^{44}Ca/^{40}Ca$ fractionation during inorganic calcite formation: II. Ca isotopes, *Geochim. Cosmochim. Acta*, *72*, 3733–3745.

Ullmann, C. V., U. Wiechert, and C. Korte (2010), Oxygen isotope fluctuations in a modern North Sea oyster (*Crassostrea gigas*) compared with annual variations in seawater temperature: Implications for palaeoclimate studies, *Chem. Geol.*, *277*, 160–166.

Ullmann, C. V., H. J. Campbell, R. Frei, S. P. Hesselbo, P. A. E. Pogge von Strandmann, and C. Korte (2013), Partial diagenetic overprint of Late Jurassic belemnites from New Zealand: Implications for the preservation potential of δ^7Li values in calcite fossils, *Geochim. Cosmochim. Acta*, *120*, 80–96, doi:10.1016/j.gca.2013.06.029.

van Beusekom, J. E. E., S. Weigelt-Krenz, and P. Martens (2008), Long-term variability of winter nitrate concentrations in the Northern Wadden Sea driven by freshwater discharge, decreasing riverine loads and denitrification, *Helgoland Mar. Res.*, *62*, 49–57.

van Beusekom, J. E. E., M. Loebl, and P. Martens (2009), Distant riverine nutrient supply and local temperature drive the long-term phytoplankton development in a temperate coastal basin, *J. Sea Res.*, *61*, 26–33.

Vander Putten, E., F. Dehairs, E. Keppens, and W. Baeyens (2000), High resolution distribution of trace elements in the calcite shell layer of modern *Mytilus edulis*: Environmental and biological controls, *Geochim. Cosmochim. Acta*, *64*(6), 997–1011.

Veizer, J., et al. (1999), $^{87}Sr/^{86}Sr$, $\delta^{13}C$ and $\delta^{18}O$ evolution of Phanerozoic seawater, *Chem. Geol.*, *161*, 59–88.

Wang, H., E. Keppens, P. Nielsen, and A. van Riet (1995), Oxygen and carbon isotope study of the Holocene oyster reefs and paleoenvironmental reconstruction on the northwest coast of Bohai Bay, China, *Mar. Geol.*, *124*, 289–304.

Zachos, J., M. Pagani, L. Sloan, E. Thomas, and K. Billups (2001), Trends, rhythms, and abberations in global climate 65 Ma to present, *Science*, *292*, 686–693.